

REACTIVITY WITHIN SMECTIC B LIQUID CRYSTALLINE PHASES

B. Samori,^a P. De Maria,^b P. Mariani,^c F. Rustichelli,^c P. Zani^a

a: Istituto di Chimica Organica
Facoltà di Chimica Industriale
Viale Risorgimento 4, 40136 Bologna (Italy)

b: Istituto di Chimica Organica
Via Archirafi 26, 90123 Palermo (Italy)

c: Istituto di Fisica Medica
Università di Ancona (Italy)

(Received in UK 16 February 1987)

Abstract - ASE quaternization reaction is used as reactivity probe within Sm B solvents. The aim of the present study was that of investigating, by means of many physical techniques (DSC calorimetry, Optical Microscopy, X-ray diffraction, Kinetic measurements and Linear Dichroism), the profound differences which occur in a reaction carried out in "internally non-homogeneous" smectic phases with respect to "internally homogeneous" media, such as isotropic, nematic or cholesteric solvents.

The Linear Dichroism technique proved particularly valuable in this regard because it displayed multisite distribution of the solute reactant molecules within the SmB solution. This observation provides a unifying framework explaining the experimental data from all the different physical techniques employed.

Despite high expectations and interest in the field of reactivity within thermotropic liquid crystalline solvents, all the researches reported by the end of the 1970s were rather frustrating and seemed to discourage hopes of notable developments in this field.¹⁻² The papers of Weiss et al.³ were the only encouraging exceptions. They opened the prospect of using thermotropic liquid crystalline solvents as a tool in the elucidation of both fluorescence quenching and reaction mechanisms. However, apart from one brief attempt^{3b} to use a Smectic (Sm) phase, these results were all obtained with Nematic (N) or Cholesteric (Ch) mesomorphic solvents.

Our feeling that the short-range orientational order of N or Ch phases is not tight enough to induce relevant stereochemical and catalytic effects grew stronger with time.⁴ It led us to probe into the reactivity within the most ordered Sm phases and, depending on the reaction under study, we exploited several Sm B solvents: ZLI-1409,^{5,6} ZLI-1544,^{5,7} ZLI-1756,⁸ OS-44,⁹ OS-53,⁹ OS-35.⁹

The strong anisotropic constraints they can exert in the conformational equilibria¹⁰ or in the diffusion properties¹¹ of the reactant solute molecules might affect the pathways of monomolecular or bimolecular reactions, respectively. We observed both effects by using as reactivity probes the monomolecular rearrangements of limonene or linalool⁸ and the bimolecular quaternization reactions of methyl- or allyl-p(dimethylamino)benzenesulfonate (MSE or ASE).^{5-7,9}

Since then Sm B media have been checked by other scientists as solvents for very different kinds of reactions and some very promising results have been obtained.^{12,13} At the same time, we have

been furthering our knowledge of the process as well as carrying out polymerization of bisacrylic monomers in Sm B solvent¹⁴ and asymmetric induction of chiral Sm C* and Sm A* solvents on episulphoxide synthesis and sulfoxides photoracemization.¹⁵ The problems encountered during these researches made it increasingly clear to us with time that our initial approach — basically suitable for studies of reactions within liquid media — ought to be more open so as to embrace and focus on similarities between our reactions and solid phase processes.

This approach was therefore adopted in our study of the ASE catalysis by Sm B solvents.

The Sm phases have a layered structure, and their constituting molecules have a fairly rigid core and flexible alkyl chains. This structure leads to an alternating sequence of sub-layers determined by the alignment in planes of the centers of gravity of adjacent cores or of adjacent tails (Figure 1).

Sm B mesophases may therefore provide a very good compromise between the reactivity in solid and liquid media. Sm mesophases are in fact able to supply very anisotropic potentials to molecular orientations,^{16,17} as can the solid phases, while they are also able to overcome the main limitation of the reactivity in solids. This limitation is due to solid state molecular diffusion so low as to often inhibit the molecular motion necessary for product formation. Soft displacements of properly oriented molecules must in fact be provided by the dynamic nature of the crystal lattice when a reaction takes place.¹⁸

The looser packing of a Sm medium, acting as orienting host, allows softer reactivity for the guest molecule. But the tight order and the strong similarity of these mesophases to solid media make the steric requirements for a guest molecule solubilization much stricter and the local order-destroying-power of the same guest molecule much higher than when N or Ch solvents are used.¹⁹

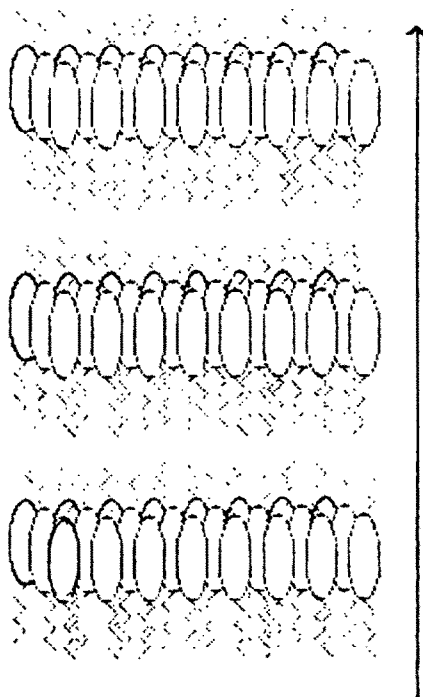
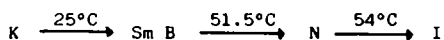
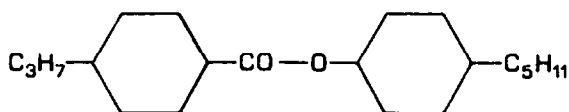


Figure 1: layered structure of Sm liquid crystalline media. The rigid-core- and alkyl-chain-sublayers are sketched by ellipsoids and tails respectively

A detailed knowledge of the reactant-solvent mixture within the "reaction-pot" is therefore necessary. Differential Scanning Calorimetry (DSC), Optical Microscopy (OM) and X-ray Diffraction (XD) are very useful in this respect as will be shown by the present study.

We used OS 35 from E. Merck (Darmstadt) as mesomorphic solvent because it provides a room temperature Sm B phase which is transparent to u.v. radiations⁹ (as the BCCN, used by Weiss^{12a} and Leigh^{13a}) and because it is without the rather reactive cyano group of CCN's.



Its transparency allowed a kinetic analysis of the ASE reaction to be carried out easily by spectroscopic methods without any previous solvent separations. It also allowed ASE orientation and location within the host Sm B phase to be studied by Linear Dichroism (LD) technique. The LD spectra offered clear evidence of the role that the structural dishomogeneity within the layered structure of Sm solvents may play in the reactant encounter processes.

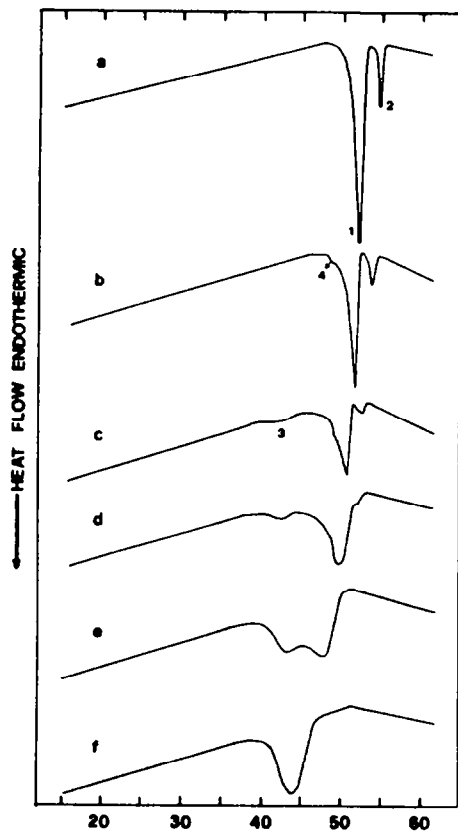


Figure 2: calorimetric curves obtained by heating OS 35 samples with different ASE concentration: (a) pure OS 35; (b) $1.05 \cdot 10^{-2}\text{M}$; (c) $2.76 \cdot 10^{-2}\text{M}$; (d) $6.19 \cdot 10^{-2}\text{M}$; (e) $10.20 \cdot 10^{-2}\text{M}$; (f) $23.86 \cdot 10^{-2}\text{M}$.

1. Thermal Analysis, Optical Microscopy and X-ray Diffraction of the reactant-solvent mixture.

DSC Thermograms on heating the mixture at increasing ASE concentrations are reported in Figure 2. The first, (a), is that of the pure solvent and shows the two peaks labelled (1) and (2), relative to the transition from Sm B to N and from N to I (isotropic) phases, respectively. The sizes of these two peaks clearly display how different is the heat associated with the two phase transitions, i.e. how low the solvent rigidity of the N phase is with respect to the Sm B. In fact the enthalpy and the entropy of a transition reflect the changes, on passing from one phase to another, in the intermolecular forces and in the molecular packing, respectively.¹

On increasing the reactant concentration in the two-component guest-host system, the temperatures of the two transitions gradually lower and their DSC peaks broaden. This is due to both the gradual loss of cooperativity in the diffusion properties of the system and the appearance of two-phase regions across the phase transitions.²⁰ In addition, a new peak (3) already starts to appear at the very low ASE concentration of thermogram (c), and its intensity increases with the ASE concentration at the expense of the other two peaks. This new peak then dominates the whole thermogram (f), which corresponds to a $24.0 \cdot 10^{-2}$ M ASE concentration. Also, a very small shoulder (4) between peaks (2) and (3) is displayed by thermograms (b) and (c). This very small signal which appears in a limited range of concentrations was confirmed by other thermal analyses of OS 35 mixtures with other solute organic molecules.

The temperatures of the maxima of peaks (1) to (4) obtained for the mixtures analyzed are reported in Figure 3. Strong hystereses were observed on cooling the mixtures down.

Optical microscopy showed that the solution is N between peaks (1) and (2), and Sm B below peak (1). The Sm B mosaic texture remained unchanged when mixtures at low ASE concentrations (lower than $2.5 \cdot 10^{-2}$ M: region I of Figure 3) were cooled down to room temperature. By contrast, region II displays changes in the Sm texture on passing from part (a) to part (b), changes which also seem to indicate the tendency of the system to give rise to a eutectic. At the highest solute concentrations, optical microscopy reveals separation of isotropic droplets within the bulk Sm B platelet texture which is probably due to a non-complete ASE solubilization.

Within the entire IIa region the overall Sm B mosaic organization is in equilibrium with both isotropic and nematic phases. Coexistence of the three phases, which is forbidden by the Gibbs phase rule, was also detected. This is not very surprising. In fact the phase rule was established for the melting of a perfect infinite crystal where all the molecules are forced together to cooperate in the transition.²¹ In our binary case the cooperative unit (i.e. the number of molecules which cooperate) will be smaller than the whole bulk owing to local structural imperfections and non-ideal mixing of the two components.

Therefore, in these cases, the Gibbs phase rule cannot be strictly applied and phase diagrams cannot be rigorously constructed. For this reason, Figure 3 only reports the mid-points of the transitions, which may thus be considered as the phase transition temperatures.

The X-ray diffraction profiles showed by OS 35-ASE mixtures are basically the same as those reported in reference 9 for the pure solvent. The interlayer and the intermolecular distances, which can be derived from the low- and high- angle peaks respectively, are not significantly affected by the ASE presence. The reactant molecules do not seem to modify the overall long-range structural organization of the sample which determines the diffraction pattern. This may be due to the fact that guest perturbations of a very tight host molecular packing have a local, very short-range effect only. The Sm B structure, characterized by a well defined separation between the aliphatic and rigid core sub-layers (Fig. 1) is in fact mostly determined by the interactions among

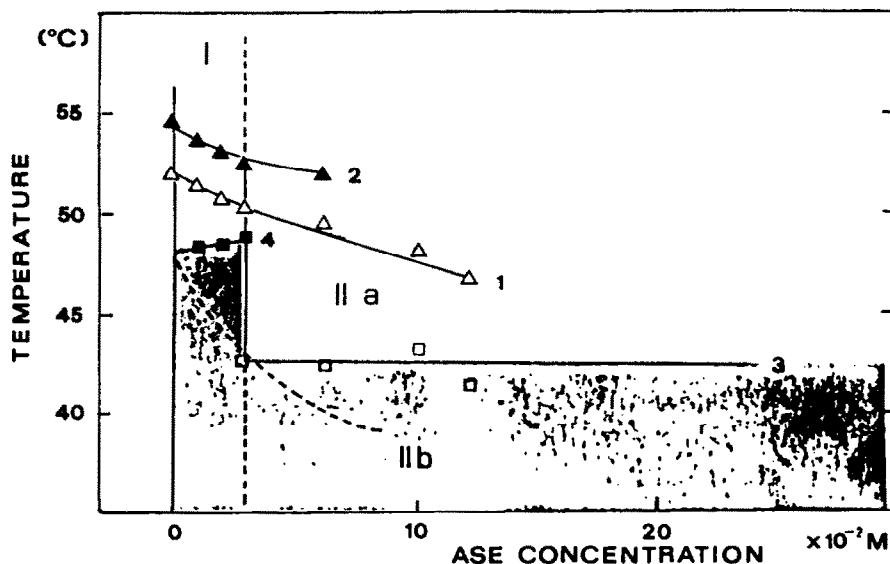


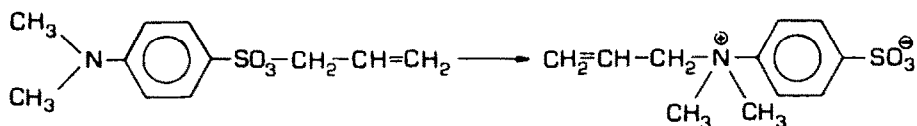
Figure 3: temperatures of the transition peaks, as labelled from (1) to (4) in the DSC thermograms in figure 2. The mesomorphic states in the different areas I, II a, II b are discussed in the text. The shaded areas display the regions of the phase diagram where the ASE quaternization takes place. This reaction is in fact blocked by the appearance of Isotropic or Nematic phases. The broken line within the area of existence of the SmB phase reports the threshold ASE concentrations for which the rate constant is still independent of total reactant concentration and after which strong rate depressions occur. This broken line therefore displays the occurrence of discontinuities in the reaction kinetic pattern within the SmB phase of the reaction mixture.

the cores.

The tails contribute poorly to the overall packing energy but play a marked role by their flexibility²² in absorbing and annihilating density defects and in dissolving non-mesomorphic solute molecules.

2. Kinetic Measurements

In the previous papers of this series^{6,7,9} we have demonstrated that the ASE quaternization is an effective probe of the occurrence of liquid crystalline catalysis.



In fact, although this reaction occurs at a detectable rate even in the melt, it is attainable neither in common (isotropic) solvents nor in the solid state. In addition, we have previously shown⁹ that, at 36°C in the Sm B phase of OS 35, this same reaction is a simple second order process and that the mechanism is most likely a dimeric SN_2 -type bimolecular pathway. However, the aforementioned new approach, i.e. the considering of this process as more closely related to the solid-state- than to the liquid-state-reactivity, requires that the kinetic investigations be strictly subordinate to the phase diagram in fig 3 and to its two variables (ASE concentration and temperature). Therefore we have been following this reaction in a as-wide-as-possible temperature interval within the Sm B phase of the solvent, and in a wide range of initial solute concentrations.

a. Temperature effects.

Kinetic measurements were carried out in the temperature interval $44^\circ\text{C} \geq T \geq 28^\circ\text{C}$. As previously observed^{6,9} k is strictly second order at each individual temperature, provided that the concentration of ASE is less than the threshold value. An Arrhenius-plot (Fig. 4) of $\log k$ vs $1/T$ shows a sharp upward curvature. Apparently $\log k$ asymptotically increases to infinity when T equals the transition Sm-N temperature of 49°C . However, because of the superimposed concentration effect (discussed below), the temperature interval $44 < T \leq 49^\circ\text{C}$ is not experimentally accessible to our kinetic technique.

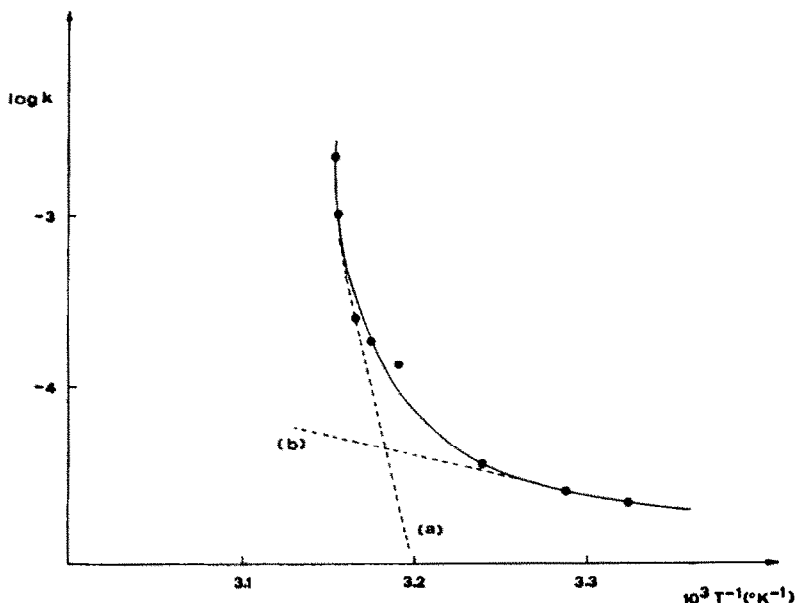


Figure 4: Arrhenius-type plot for the ASE quaternization in OS 35 SmB phase at concentrations lower than the temperature-dependent threshold values. (see text and fig.5). Lines (a) and (b) are hypothetical straight Arrhenius extrapolations of the higher and lower temperature data, respectively.

The very remarkable curvature of this Arrhenius plot may imply strong temperature effects upon the reaction sites revealed by the LD technique (see below) within the Sm mesophase.

We may look at the plot in Figure 4 in terms of positive deviations at lower temperature with respect to a hypothetical Arrhenius straight line (a). Or, we may also think in terms of positive deviations at higher temperatures with respect to line (b). The concave shape of the curve is assured by a non-linear dependence of the collision factor in A and/or the activation energy E_a upon temperature.

It must also be pointed out that the Arrhenius curve does not display any discontinuity at the ASE melting point temperature (40°C). This therefore rules out any significant role played by local reagent segregations out of the solution. In fact ASE reactivity in a diluted Sm B solution was found to be drastically different from that in its pure melt phase.

The very significant kinetic comparison in table 1 should also be emphasized. It shows that, despite the low concentration of the reactant solute, the Sm solvent is able to induce rate accelerations with respect to the ASE conversion in its pure melt phase. This is a further clear-cut evidence that the liquid crystalline catalysis we observed cannot be ascribed only to solute bulk aggregation out of the solution. The next reported LD data confirm, furthermore, that the solute is

still oriented and dissolved by the solvent within and throughout the Sm B phase. The temperature effect on the threshold concentration (see below) also rules out any relevant role played by ASE segregation processes.

Table 1. Conversion yield of ASE quaternisation at 44.0 C in OS-35 Smectic B liquid crystal and in the melt ph.

| time (days) | Percent conversion | |
|-------------|--------------------|------------|
| | L.C. | Melt phase |
| 1 | 67 | 15 |
| 5 | total | |
| 26 | total | |

b. Concentration effects.

As mentioned above, the second order rate constant k at "high" initial concentration of ASE is by no means independent on total solute concentration. It sharply decreases beyond a definite concentration value which, in turn, depends on temperature. The dependence of k on concentration at 40°C is graphically represented in Figure 5. We have evidence that the concentration value at which rate depression starts (threshold concentration) dramatically decreases with increasing temperature. All these kinetic data will be presented and discussed in full detail in a separate paper.²³

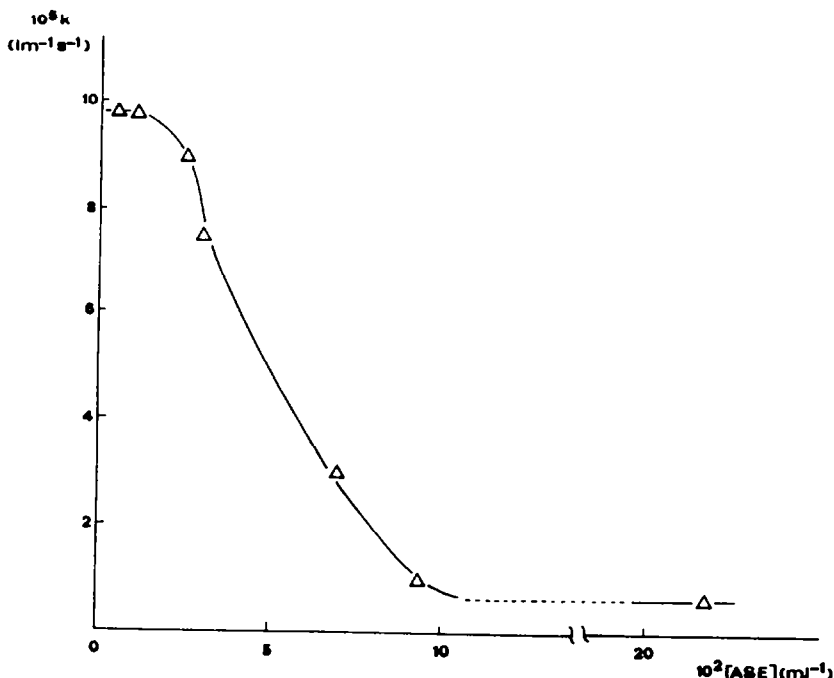


Figure 5: dependence of the kinetic constant on the solute concentration at 40 °C. The threshold value at which rate depression starts and the second order constant becomes dependent on total solute concentration is clearly displayed.

By combining the DSC calorimetric data and the kinetic measurements, it is possible to relate reactivity to the mesomorphic status of the reactant mixture. It must be taken into account that the experiments were not carried out under strictly comparable conditions, i.e. the calorimetry

measurements do not correspond to an equilibrium condition²⁴ while the kinetic do. In spite of this, it should be pointed out that the process under investigation seems to occur only in the shaded area in Figure 3's phase diagram of the reacting mixture.

The broken line reported in the same area is a tentative evaluation of the temperature dependence of the threshold concentration at which a dramatic rate depression occurs. This is considered an estimation because of the few data available and the difficulty in getting them.²³

The broken line limits the temperature - ASE concentration area where the second order rate constant is still independent of total solute concentration.

In summarizing the Kinetic and the DSC data together it may be pointed out that:

- ASE quaternizes more slowly in its pure melt phase than in a very diluted Sm B solution (Table 1).
- The Arrhenius plot of the reaction has a very unusual and remarkable upward curvature (Fig 4).
- The maximum values of ASE concentration, for which the rate constant is still independent of total ASE concentration and after which strong rate depressions occur, decrease with increasing temperatures (Fig 3). This effect leads to further boundaries to the reactivity also within the Sm B phase of the solution.
- The reaction is also blocked by the appearance of I or N phases within the phase diagram of the reaction mixture (Fig. 3).

3. Linear Dichroism Investigation of the Reacting Mixture.

A sample is said to exhibit L.D. if it absorbs light to different degrees depending on its linear polarization. The L.D. is usually defined as the differential absorption $|E_{||}(\lambda) - E_{\perp}(\lambda)|$ of two plane-polarized components of an electromagnetic radiation, where parallel ($||$) and perpendicular (\perp) are referred to the optical axis, or director, of the oriented sample (i.e. the direction of the electric or magnetic orienting field). $[E_{||}(\lambda) + E_{\perp}(\lambda)]/2$ is the Average Absorption (A.A.) of the same oriented sample. L.D. and A.A. spectra may be directly recorded by modulated techniques,⁶ e.g. by using a dichrograph which may be switched from one measurement to the other without touching the sample.

For a band purely polarized along the u-direction:

$$\frac{|E_{||}(\lambda) - E_{\perp}(\lambda)|}{|E_{||}(\lambda) + E_{\perp}(\lambda)|} = \frac{3 S_{uu}}{2 + S_{uu}} \quad \text{where } S_{uu} = \frac{1}{2} (3 \cos^2 \beta - 1)$$

The distribution of deflections β of the transition moment u directions of all the guest absorbing molecules from the sample director determines the shape and signs of the resulting L.D. spectrum. The S_{uu} function, averaged ($\langle \dots \rangle$) over all the transition moment orientations, is an order parameter with values of zero or one for random orientation or perfect-alignment, respectively. If the polarization of the investigated transitions is known, information about the guest molecule orientation can be obtained and expressed in terms of S_{uu} values.

The lowest energy ASE electronic band, which is centred at 277 nm, is due to a charge transfer (CT) transition from the donor amino group to the sulphonate acceptor, and it is therefore polarized along the molecular long axis.

We have reported in a previous paper⁶ an LD spectrum of ASE within the N and Sm phases of a BCCN mixture (ZLI-1167) which was macroscopically oriented by applying an electric field to the sample.

Taking advantage of the transparency to UV-light and to the diamagnetic anisotropy of the reaction solvent (OS 35) itself in order to run LD spectra at different temperatures and ASE concentrations, we developed a new set up for the LD technique. The orientation was achieved by applying a magnetic field to the samples in their N ranges and then slowly (about $0.05^{\circ}\text{C min}^{-1}$) cooling them down to their Sm range.

Figure 6a shows the profiles of the LD bands, corresponding to the B_{2u} absorption of the ASE molecules, obtained on cooling the samples from the I ($T > T_n$) down to the Sm phase ($T < T'_s$). The state of the samples was always kept under control by either visual inspection or microscope observation during the complete temperature scanings and the spectroscopic investigations.

Obviously no orientation can be achieved in the I range of the mesomorphic solution, and only at T_n when the first droplet of a N phase starts growing on the light path, does the LD start to come out. The profile (1) corresponds to this first appearance of the N phase. The signal increases because of the gradually increasing amount of the N phase on the light path during the I-N transition and also because of the tightening up of the N order with decreasing temperature. But, suddenly at T_s , when the Sm B phase appears, the signal collapses till T'_s at which the solution appears to be completely Sm. The system is still able to respond to the orienting field by increasing its overall orientation while decreasing the temperature. The strong signals of the profiles (5) and (6) were obtained within the Sm B phases at $T < T'_s$.

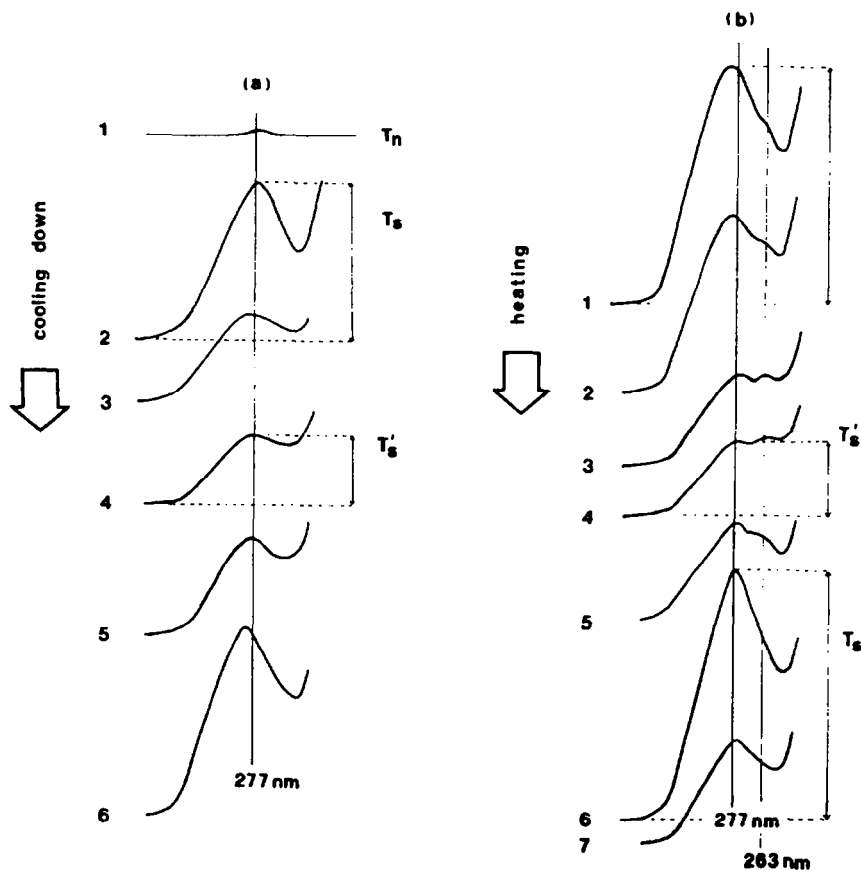


Figure 6: profiles of the $[E_{||}(\lambda) - E_{\perp}(\lambda)]$ Linear Dichroism bands of a reaction mixture oriented by a magnetic field (12 KG) on cooling down (a) or heating up (b). The temperature T_n corresponds to the first appearance of the Nematic on cooling from the Isotropic phase; T_s and T'_s to the points at which the Nematic to SmB transition starts and is completed, respectively. The Linear Dichroism signals, which are usually reported as $[E_{||}(\lambda) - E_{\perp}(\lambda)]$, are therefore negative in this case.

By this technique it may also be possible in principle to follow the local orientation of both the mesomorphic host and the reactant guest molecules on changing temperature and relative concentration of the solute-solvent system. This can be achieved if a spectral region is available where no overlapping occurs between the solute and solvent absorption. Unfortunately, this is not the case because the LD signal at 243 nm, out of the ASE absorption, is determined both by solute and solvent absorptions and their orientations.

The ASE concentration range which may be spanned by this technique is determined by the solute's molar extinction coefficient ($\epsilon_{\max} = 25850$ in aqueous ethanol 3:2 v/v) together with the cell pathlength. Because of these restrictions, we prepared a $4.28 \cdot 10^{-4}$ M solution (or 10^{-4} ASE/OS 35, W/W) for the LD study. In order to investigate as well the effect of increasing solute concentration on the orienting ability of the solvent and the guest location, small quantities of methylcyclohexane, which does not absorb the UV light, was injected into the ASE solution up to a $10^{-2} - 10^{-1}$ M total concentrations of the two solutes.

LD spectra were recorded for the different solutions with or also without annealing procedures at the N-Sm transitions.

Figure 7 sketches the behaviour of the LD signal intensity displayed (on cooling the samples down) by the ASE transition at 277 nm. This sort of sigmoidal plot was displayed by all the experiments carried out on cooling from the isotropic phase ($T > T_n$) down to the Sm phase ($T < T'_s$). The LD intensities and the temperatures T_n , T_s , T'_s corresponding to the curve inversion points are variously shifted in the temperature scale on changing the solute concentrations in the investigated samples. The LD intensities within the Sm phase also depend on the thermal history of the sample within the magnetic field, i.e. on the annealing cycles carried out at the N-Sm transition.

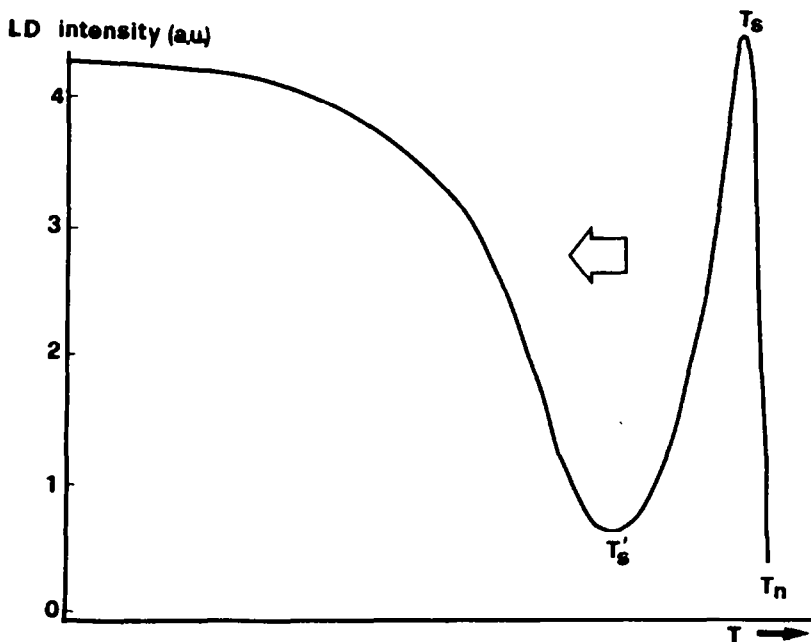


Figure 7: sketch of the behaviour of the Linear Dichroism signal intensity displayed (on cooling the samples down) by the ASE transition at 277 nm. The shape of this sort of sigmoidal plot is affected by solute concentrations and annealing cycles carried out at the Nematic-Smectic transitions.

Several important differences appear during the heating up part of the temperature scanning cycle. The general trend of figure 7 is basically preserved even if at $T < T'_s$ the slopes of curves do not reproduce those of the corresponding ones obtained on cooling down: strong hysteresis was observed. Figure 6b reports the LD profiles which reveal something completely new that was not previously observed during the cooling-down part of the cycle. A new LD band, centred at 263 nm, increases with temperature with respect to the "normal" band at 277 nm till T'_s . This new band then disappears completely at T_s when the Sm phase disappears, too.

These double-humped spectrum may be explained by a solute distribution among at least two different solubilization sites. Different solvation environments may cause two signals to appear widely apart from each other. The transition under investigation has a strong charge-transfer (CT) character and therefore is characterized by a strong tendency to reveal changes in the polarity and the solvation within the environment by large energy shifts.

The sample absorption spectrum which was recorded at the same time (see figure 8) reveals another detail of this multisite distribution, i.e. the band is centred at 277 nm and does not show any other band or shoulder in correspondence to this new LD peak. This new LD peak falls in an area where the absorption spectrum has a deep throat. Therefore most of the guest molecules are in the solvation site which gives rise to the lower-energy LD maximum. The remaining small amount of molecules in the other site are revealed only by the LD shoulder at higher energy because of their much higher S_{uu} order parameter.

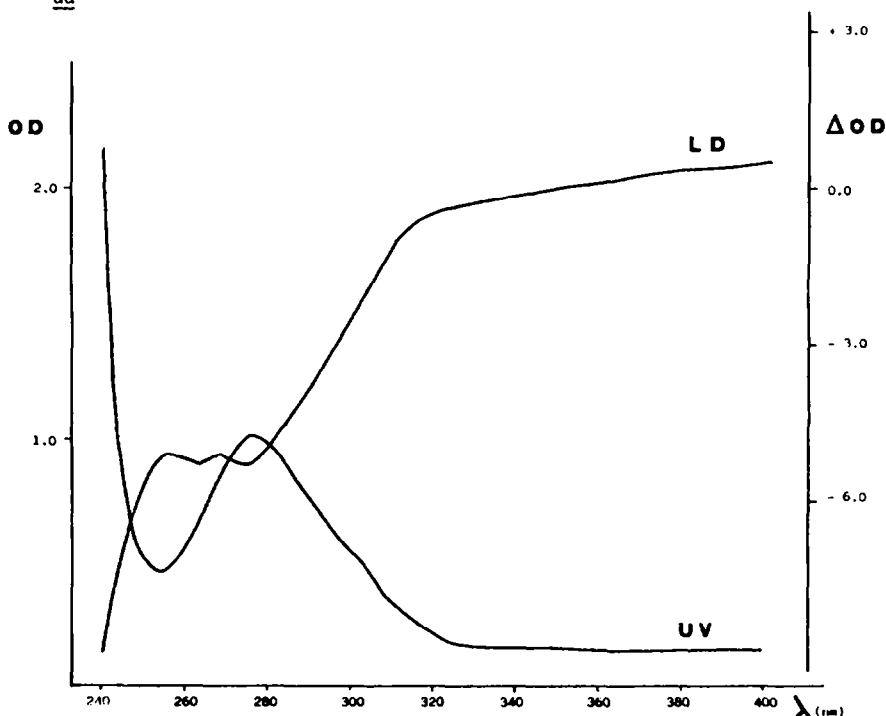


Figure 8: profiles of the Linear Dichroism and relative isotropic Absorption of an oriented sample which displays the solute location within two different sites.

Being the ASE transition, which we are looking at, polarized along the long-molecular-axis, the constant negative sign of its L.D. displays that, in both the N and Sm phases, the guest ASE molecules tend to align their long molecular axes to those of the surrounding host mesomorphic molecules. The negative diamagnetic anisotropy of the latter forces their long molecular axes to

stay preferentially on planes perpendicular to the magnetic field (Fig. 9). A perfect molecular alignment may be sketched by limiting orientations (a) and (b) (in Figure 9) which, in this case, can be considered to be equally populated, in absence of other orienting forces such as surface effects. The annealing procedures at the N-Sm transition improve the orientation within the Sm phase: the instantaneous orientation which is achieved by the field in the N phase may be gradually transferred to the more viscous and hard-to-orient Sm phase, while its layered structure is enucleating at the transition. The layer enucleation process leads to a decrease of the overall orientation of the molecules with respect to the magnetic field and, therefore, it is responsible for the collapse of the LD signal between T_s and T_s' .

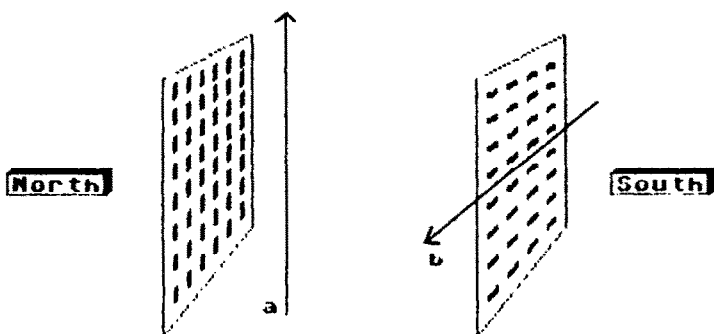


Figure 9: limiting orientation modes of molecules (as OS 35) with negative diamagnetic anisotropy within a magnetic field. The long axis tends to stay perpendicular to the orienting field, thus leading to equal population of the two limiting orientation modes (a) and (b).

The highest LD peaks achieved at $T < T_s'$ within the Sm phases were always lower than those of the N ones, despite the well-known higher local order of the Sm layered structure. However the LD gives an estimation of the overall molecular alignment with respect to a director, which provides linear anisotropy to the sample along the direction of propagation of the incoming polarized beam. The lower overall anisotropy of the Sm sample for LD measurements is mostly due to surface effects which force the Sm layers to grow parallel to the cell windows, as shown by OM observations. The molecular long axes of both guest and host molecules are forced to stay perpendicular to the mesomorphic film under investigation. ASE's long axis transition moment is aligned to the direction of the beam's propagation and does not contribute to the sample's overall linear anisotropy and to its light absorption. The LD signals are therefore determined only by the (a)-like components of the transition moments.

In summary, the LD measurements revealed that:

- a) The reactant ASE molecules tend to align their long molecular axes to those of the surrounding host OS 35 mesomorphic molecules.
- b) The ASE molecules are located within two different sites of the host Sm B structure.

c) The population and the local order of the two sites are very different. The site corresponding to the LD band at about 263 nm is much less populated but much more ordered than the site displayed by the LD band at about 277 nm.

CONCLUSIONS

Sm B solvents provide the most efficient way to carry out ASE rearrangement.

We have said⁶⁻⁹ that this result may be interpreted "in terms of the ability of the mesomorphic solvent to drastically affect the free energy of activation of this reaction by exerting anisotropic restraints on the dynamic properties of the reactant molecules." But this sentence, which may be actually applied to all reactions within all mesomorphic solvents, was found by the present study to be too vague and general in terms of Sm solvents.

The Sm B phase, in particular, offers a very good compromise between the reactivity in solid and the reactivity in liquid or nematic media. The picture of the Sm B phase is in fact that of "a plastic lamellar crystal, with 3-dimensional positional order and rotational disorder, and an easy direction of slip parallel to the layers".²⁷ This could also mean that the reactivity in Sm B solvents may be more closely related to solid- than to liquid-state processes. The aim of the present study was therefore that of revealing, by as many physical techniques as were available to us, the profound differences brought about in a reactive process by Sm B solvents with respect to the same process in I or even in N media. These differences are basically determined by the non-homogeneous internal structure of the Sm solvent, i.e. its alternating sequence of layers with a liquid-like (alkyl chains) or crystal-like (rigid cores) packing leads to very peculiar and complex solubilization equilibria of the guest reactant molecules within different location sites.

This paper clearly shows that studies in this field must always rely on a thorough knowledge of the specific solubilization processes which take place within the reactive mesomorphic solution. In fact, the ASE reaction, which was carried out by us in different solvent's mesophases, showed discontinuities (Figs 3 and 5) in its kinetic pattern which were not necessarily due to phase transitions or structural modifications of the solution's mesomorphic state. It has already been demonstrated by us that the reaction rate collapses at the first appearance of a N or I phases.⁶ These phases are likely to be able to dissolve greater amounts of the reactant than the Sm ones but not to drive the reaction towards a significant product formation.⁶⁻⁹ Moreover, this paper shows that, even within the area of existence of the Sm B phase, the reaction's kinetic pattern evinces discontinuities with temperature and solute concentration (Fig. 3 and 5) and a strongly concave Arrhenius plot.

The valuable LD evidence of at least two solubilization sites of the reactant molecules within the mesomorphic solvent may offer an interpretive key to all these kinetic data.

The two types of sites are likely provided by the rigid core layers and by the regions of the more flexible alkyl chains. Solute expulsion processes, within Sm solvents, from the cores to the chain layers were already suggested by ESR,²⁸ NMR^{11,29} and Fluorescence³⁰ measurements. But the LD spectra in Figures 8 and 9 provided the clearest evidence of these equilibria by displaying a separate signal for each of the two sites. The site revealed by this technique to be the more ordered and far less populated than the other is likely provided by the cores. This reaction site is probably also the less reactive one: its crystal-like packing may prevent the molecular diffusion within the core-layers necessary for the encounters of the reagent molecules and for

product formation.¹¹

The reactant jumping between the two sites is fast compared to the rate determining bimolecular process. The partition of the reactant molecules between the two sites leads to a sort of pre-equilibrium-type situation with relative populations which are strongly dependent upon temperature, as the LD profiles in Figure 8 suggest. The positive deviations which determine the remarkable upward curvature of the Arrhenius plot in Figure 4 may be due to a temperature effect on the population of the more reactive site.

This temperature-dependent partition of the solute between sites in rigid core and in aliphatic tail layers may also explain the observed temperature effect on the threshold concentration and the kinetic discontinuities (Fig 3 and 5) within the solution Sm B phase. In fact the order of the rigid core layers was observed to remain practically constant within the whole temperature range of the Sm B phase.^{31,22} In fact the range of existence of this phase is mostly determined by the tightly-ordered packing of the cores. By contrast the flexibility of the aliphatic tails is likely to be more temperature-dependent, as also suggested by the large activation energy recently obtained by Selwyn *et al.*²⁹ for the reorientation motions of a solute probe within a Sm B phase. In increasing temperature, the local order the host aliphatic tails provide for the guest reaction to take place may therefore disappear before the Sm → N transition and at very low ASE concentrations, as to give rise to the kinetic discontinuities observed within the range of existence of the solution's Sm B phase.

These discontinuities may not be due to solute segregation processes out of the solution as its solubility is expected to increase with temperature. Solute segregation processes were in fact only observed (even at the OM) by lowering temperature and greatly increasing solute concentration.

EXPERIMENTAL

Materials

Allyl p-dimethylaminobenzenesulphonate (ASE) was prepared by a modification of the reported³³ procedure:

Allyl alcohol (21.5 g., 0.37 mol) was allowed to react with powdered NaOH (0.12 g., 3 mmol). When dissolution was almost complete, an ethereal solution of p-dimethylaminobenzenesulphonylchloride³³ (0.55 g., 2.5 mmol) was added. The resulting solution was stirred at 0°C during 1 h. After 12 h in the refrigerator, the solvent and the unreacted alcohol were removed in vacuo and the solid residue was extracted with diethyl ether. The salts were filtered off and the filtrate was dried (Na₂SO₄). Evaporation gave a crude product which was further crystallized from petroleum ether² (b.p. 40–60°C), giving pure ASE (0.38 g., 65% yield on sulphonyl chloride), m.p. 40–41°C. The liquid crystals employed in the present investigation are now commercially available materials; OS 35 was supplied by E. Merck (Darmstadt).

Techniques

The D.S.C. measurements were carried out on a Perkin Elmer Calorimeter Model DSC-2. scan rate was 1°C/min. Aluminium containers of 20 μl capacity were used.

Optical microscopy was performed with a polarizing microscope (Leitz Ortolux 2 Pol) equipped with a Mettler FP 52 hot-stage. Scan rates of 1°C/min were used during the heating and of 0.2°C/min during the cooling.

X-ray diffraction: goniometric scans were obtained by using a conventional powder diffractometer. Ni-filtered Cu-K_α radiation ($\lambda = 1.54 \text{ \AA}$) was used. The divergence of the primary beam impinging on the sample was $\approx 8'$. The generator-sample distance was $\approx 18 \text{ cm}$ and the sample counter distance 20 cm. The sample had thickness of $\approx 1.5 \text{ mm}$ and was sandwiched between the two very thin Al sheets fixed to a circular hole in an Al matrix with diameter of $\approx 1 \text{ cm}$. Heating was obtained by a hot stage containing electrical resistors, whose temperature was controlled to 0.1°C by a BT 300/301 control system supplied by SMC, Grenoble (France). Pictures were obtained by a Marconi-Elliot toroidal camera using the same radiation emerging from a Rigaku-Denki rotating anode generator. Similar sample holders were employed to those used in the diffractometer. The heating and cooling

rates were 1°C/min.

The kinetic measurements will be described in more details in ref. 23: the general procedure employed can be summarized as follows: ASE was dissolved in the OS 35 solvent (0.1 g. samples) at 50°C by quick injections of volumes of a diethyl ether solution of known concentration. After complete evaporation of the ether, the homogeneous solution of ASE was rapidly cooled down into its Sm B phase by immersion in a bath thermostatted at the desired temperature. Portions (ca. 0.01 g) of the reaction mixture were taken at appropriate intervals and the reaction quenched by dilution with RS-grade ethanol (5 ml). The absorbance of these ethanolic solutions of ASE was determined with a Beckmann DU or a Varian spectrophotometer at $\lambda = 284 \text{ nm}$.

The LD and UV spectra were recorded by a JASCO-J500 dichrograph and by a JASCO UVIDEC-610 spectrophotometer.

The modulated technique used for recording L.D. allows the UV spectra to be recordered by the dichrograph on the same sample without touching anything but a selector to switch from L.D. to absorption measurement. This is particularly important because, on changing instrument or even sample orientation, the investigated area may be different, as the concentration of the molecules on the light beam may do. The liquid crystal linear dichroism (L.C.L.D.) technique is described in ref. 26. In this case, instead of the electric field or surface treatment previously used, we have been orienting the sample with a magnetic field (12 KG) generated by an electromagnet placed in the cell compartment of the dichrograph with the magnetic field perpendicular to the light beam direction. This is not the Magnetic Circular Dichroism (MCD) classical orientation and the electromagnet was modified to provide this possibility. The sample temperature was carefully controlled by thermostatted water circulating in a compartment surrounding almost the whole cell, which was expressly built to this purpose by Starna Ltd (Romford, Essex, U.K.): the cell design was as follows: a rectangular quartz cell (optical path 1 mm) was sealed in a quartz chamber having two open windows along the light path and carrying two connections for a circulating fluid.

ACKNOWLEDGEMENTS

This intriguing problem of the reactivity in Sm B phases was the subject of many helpful discussions with Profs. C. Zannoni, G. Gottarelli and G. Maccagnani (Bologna), and Prof. G.W. Luckhurst (Southampton). We thank also E. Merck (Darmstadt) for supplying samples of the liquid crystal.

REFERENCES

1. Dewar, M.J.S.; Mahlovsky, B.D. J.Am.Chem.Soc. **1974**, 96, 460.
2. a. Bacon, W.E. Pramana Suppl. **1975**, 1, 455 and references therein.
b. Bacon, W.E.; Jim, Ling Kuo; Brown, G.H. Mol.Cryst.Liq.Cryst.(Lett.) **1979**, 56, 13.
c. Bacon, W.E. J.Phys. (Paris) **1975**, 36, C-1 409.
d. Aviv, G.; Sagiv, J.; Yogev, A. Mol.Cryst.Liq.Cryst. **1976**, 36, 349.
3. a. Nerbonne, J.M.; Weiss, R.G. J.Am.Chem.Soc. **1978**, 100, 5953.
b. Nerbonne, J.M.; Weiss, R.G. ibid. **1979**, 101, 402.
c. Anderson, V.C.; Craig, B.B.; Weiss, R.G. ibid **1981**, 103, 7169.
d. Anderson, V.C.; Craig, B.B.; Weiss, R.G. ibid **1982**, 104, 2972.
4. Gottarelli, G.; Samori, B. in "Liquid Crystals"; S. Chandrasekhar Ed.; Heiden & Sons: London, Philadelphia, Rheine. 1980; pp. 505-14.
5. Part 1: Samori, B.; Fiocco, L. J.Am.Chem.Soc. **1982**, 104, 2634.
6. De Maria, P.; Lodi, A.; Samori, B.; Rustichelli, F.; Torquati, G. J.Am.Chem.Soc. **1984**, 106, 653.
7. Albertini, G.; Rustichelli, F.; Torquati, G.; Lodi, A.; Samori, B.; Poeti, G. Nuovo Cimento Soc.Ital.Fis.; D,2D **1983**, 1327.
8. Melone, S.; Mosini, V.; Nicoletti R.; Samori, B.; Torquati, G. Mol.Cryst.Liq.Cryst. **1983** 98, 399.
9. De Maria, P.; Mariani, P.; Rustichelli, F.; Samori, B. Mol.Cryst.Liq.Cryst. **1984**, 116, 115.
10. a. Pedulli, G.F.; Zannoni, C.; Alberti, A. J.Magn.Res. **1973**, 10, 372.
b. Samori, B. J.Phys.Chem. **1979**, 83, 375.
c. Loewenstein, A.; Brennan, M. ibid, **1980**, 84, 340.

11. a. Vaz, N.A.P.; Doane, J.W. J.Chem.Phys. **1983**, 79, 2470.
b. Meirovitch, E.; Broido, M.S. J.Phys.Chem. **1984**, 88, 4316.
c. Moro, G.; Nordio, P.L.; Segre, U. Chem.Phys.Lett. **1984**, 105, 440.
d. Moseley, M.E.; Loewenstein, A. Mol.Cryst.Liq.Cryst. **1982**, 90, 117.
12. a. Hrovat, D.A., Lin, J.H., Turro, N.J., Weiss, R.G. J.Am.Chem.Soc. **1984**, 106, 5291.
b. Hrovat, D.A., Lin, J.H., Turro, N.J., Weiss, R.G. ibid. **1984**, 106, 7033.
c. Anderson, V.C.; Weiss, R.G. ibid **1984**, 106, 6628.
13. a. Leigh, J.W. J.Am.Chem.Soc., **1985**, 107, 6114.
b. Leigh, J.W. Can.J.Chem. **1985**, 63, 2736.
14. Mariani, P.; Samori, B.; Angeloni, A.S.; Ferruti, P.; Liq.Cryst., in the press.
15. Finzi, L.; Maccagnani, G.; Masiero, S.; Samori, B.; Zani, P. to be published.
16. Meirovitch, E.; Ignier, D.; Ignier, E.; Moro, G.; Freed, J.H. J.Chem.Phys. **1982**, 77, 3915.
17. Leadbetter, A.J. Conf.Ser.-Inst.Phys. (Neutron Its Appl.) **1983**, 64, 277.
18. Gavezzotti, A. J.Am.Chem.Soc. **1983**, 105, 5220.
19. This is displayed by the higher entropy changes during the N-Sm than the N-I transition on increasing the solute concentration (see fig 2).
20. Croucher, M.D., Patterson, D. J.Chem.Soc., Faraday Trans. 1, **1981**, 1237.
21. Lee, A.G. Biochim.Biophys.Acta **1975**, 413, 11.
22. Barbarini, F.; Chausse, J.P.; Fabre, C.; Germain, J.P.; Deloche, B.; Charvolin, J. J.Phys. (Paris) **1983**, 44, 45.
23. De Maria, P.; Tampieri, A.; Samori, B.; Zani, P. to be published.
24. Albertini, G.; Fanelli, E.; Guidoni, L.; Ianzini, F.; Mariani, P.; Rustichelli, F.; Viti, V. Int.J.Radiat.Biol.Relat.Stud.Phys. **1985**, 48, 785.
25. Birecki, H. in "Liquid Crystals and Ordered Fluids", A.C. Griffin and J.F. Johnson Eds, Plenum **1984**, pp 853-63.
26. a. Samori, B.; Mariani, P.; Spada, G.P.; J.Chem.Soc.,Perkin Trans. 2 **1982**, 447.
b. Samori, B.; Mol.Cryst.Liq.Cryst. **1983** 98 385.
27. Durand, G. Journal de Chimie Physique **1983**, 80, 119.
28. Meirovitch, E.; Freed, J.; J.Phys.Chem. **1980**, 84, 2459.
29. Selwyn, L.S.; Vold, R.R.; Vold, R.L. Mol.Phys. **1985**, 55, 287.
30. Subramanian, R.; Patterson, L.K.; Levanon, H. Photochem.Photobiol. **1985**, 41, 511
31. Hsi, S.; Zimmermann, H.; Luz, Z.; J.Chem.Phys. **1978**, 69, 4126.
32. Galbiati, E., Zerbi, G. J.Chem.Phys. **1986**, 000.
33. Sukenik, C.N.; Bonapace, J.A.P.; Mandel, N.S.; Lan, Pui-Yen; Wood, G.; Bergman, R.G. J.Am.Chem.Soc., **1977**, 99, 851.